HEPATOLOGY, VOL. 0, NO. 0, 2021

Phosphorylation and Stabilization of PIN1 by JNK Promote Intrahepatic Cholangiocarcinoma Growth

Alessio Lepore,[1*] Pui Man Choy,[2*] Nathan C.W. Lee,[1] Maria Annunziata Carella,[3] Rosy Favicchio,[4] Marco A. Briones-Orta,[2,5] Shannon S. Glaser,[6] Gianfranco Alpini ,[7] Clive D'Santos,[8] Reuben M. Tooze,[1] Mihaela Lorger,[1] Wing-Kin Syn,[2,9-11] Athanasios Papakyriakou ,[12] Georgios Giamas ,[13] Concetta Bubici ,[3**] and Salvatore Papa [1,2**]

BACKGROUND AND AIMS: Intrahepatic cholangiocarcinoma (ICC) is a highly aggressive type of liver cancer in urgent need of treatment options. Aberrant activation of the c-Jun N-terminal kinase (JNK) pathway is a key feature in ICC and an attractive candidate target for its treatment. However, the mechanisms by which constitutive JNK activation promotes ICC growth, and therefore the key downstream effectors of this pathway, remain unknown for their applicability as therapeutic targets. Our aim was to obtain a better mechanistic understanding of the role of JNK signaling in ICC that could open up therapeutic opportunities.

APPROACH AND RESULTS: Using loss-of-function and gain-of-function studies *in vitro* and *in vivo*, we show that activation of the JNK pathway promotes ICC cell proliferation by affecting the protein stability of peptidyl-prolyl cis-trans isomerase NIMA-interacting 1 (PIN1), a key driver of tumorigenesis. PIN1 is highly expressed in ICC primary tumors, and its expression positively correlates with active JNK. Mechanistically, the JNK kinases directly bind to and phosphorylate PIN1 at Ser115, and this phosphorylation prevents PIN1 mono-ubiquitination at Lys117 and its proteasomal degradation. Moreover, pharmacological inhibition of PIN1 through all-trans retinoic acid, a Food and Drug Administration–approved drug, impairs the growth of both cultured and xenografted ICC cells.

CONCLUSIONS: Our findings implicate the JNK-PIN1 regulatory axis as a functionally important determinant for ICC growth, and provide a rationale for therapeutic targeting of JNK activation through PIN1 inhibition. (Hepatology 2021;0:1-19).

Intrahepatic cholangiocarcinoma (ICC) is a tumor of the bile ducts within the liver that arises primarily from an uncontrolled proliferation of transformed cholangiocytes. With a global increasing incidence and mortality rates, ICC represents the second-most-frequent primary liver tumor after HCC.[1-3] Currently, there are no curative chemotherapies for ICC, and efforts to develop molecular-targeted therapies have been limited due to the lack of a detailed understanding of the molecular mechanisms underlying the disease.[2]

ICC usually develops in the context of both chronic inflammation of the biliary tract and liver injury that foster the accumulation of genetic mutations

Abbreviations: APL, acute promyelocytic leukemia; ATRA, all-trans retinoic acid; CHX, cycloheximide; CIP, calf intestinal alkaline phosphatase; EV, empty vector; GST, glutathione S-transferase; ICC, Intrahepatic cholangiocarcinoma; IP, immunoprecipitation; IPTG, isopropyl-β-D-thiogalactoside; JNK, c-Jun N-terminal kinase; JNK1^{CA}, JNK1 constitutive active; JNK2^{CA}, JNK2 constitutive active; KA, kinase assay; MAPK, mitogen-activated protein kinase; MD, molecular dynamics; NS, nonspecific; PD, pulldown; PDAC, pancreatic ductal adenocarcinoma; Phos-tag, phosphate-affinity gel electrophoresis; PIN1, peptidyl-prolyl cis-trans isomerase NIMA-interacting 1; p-JNK, phosphorylated JNK; PPIase, peptidyl-prolyl cis-trans isomerase; rPIN1, shRNA-resistant PIN1; SASA, solvent-accessible surface area; shJNK1/2, JNK1/2 shRNA; shNS, nonspecific shRNA; shPIN1, PIN1 shRNA; shRNA, short hairpin RNA; TMA, tissue microarray; WB, western blot; WT, wild type.

Received November 30, 2020; accepted May 16, 2021.
Additional Supporting Information may be found at onlinelibrary.wiley.com/doi/10.1002/hep.31983/suppinfo.
**These authors contributed equally to this work.*
***These authors contributed equally and jointly supervised this work.*
Supported by research grants from 250 Great Minds University Academic Fellowship University of Leeds, AMMF Cholangiocarcinoma Charity, and Foundation for Liver Research (to S.P.); Brunel Research Initiative & Enterprise Fund (LBL348) and Brunel University London (to C.B.); and in part by research grants from Blood Cancer UK (17014) (to S.P., C.B., and R.M.T.), Rosetrees Trust (M894 to S.P. and C.B.), and Guts UK (DGO2019_02 to S.P. and C.B.).

in proto-oncogenes and tumor suppressors, such as KRAS and p53, which in turn lead to the constitutive activation of signaling pathways involved in cell proliferation.[4-7] One of the major signaling pathways that are activated by mutant KRAS in ICC models is the c-Jun N-terminal kinase (JNK) signaling,[8] a member of the mitogen-activated protein kinase (MAPK) family.[9-11] Activation of JNK signaling facilitates the development of ICC by promoting the hyperproliferation of transformed bile duct cells.[8] Although the pharmacologic inhibition of the JNK kinase activity impairs the development of ICC in several mouse models of liver injury,[8] active JNK is a challenging protein to target, due to its physiological and cell type–specific functions in the liver.[12-15] Therefore, we sought to obtain a better understanding of the mechanisms by which active JNK signaling promotes ICC, because the identification of the major downstream effectors of the JNK/MAPK pathway could lead to the development of much-needed molecular-targeted therapeutics.

A key downstream effector of the oncogenic KRAS signal is PIN1, an evolutionarily conserved peptidyl-prolyl *cis-trans* isomerase (PPIase). PIN1 catalyzes the *cis-trans* isomerization of peptidyl-prolyl bonds in phosphorylated Ser/Thr-Pro motifs of the target proteins.[16-21] Through its PPIase activity, PIN1 affects the function of a large and diverse array of phosphorylated target proteins, including oncoproteins and tumor suppressors.[18-24] PIN1 is frequently highly expressed in human cancers, and its expression correlates with poor patient prognosis.[20,24] For instance, PIN1 is overexpressed in invasive ductal carcinoma breast cancer, and cooperates with activated JNK and oncogenic RAS in promoting deregulated cell proliferation by increasing the expression of the cell cycle regulator cyclin D1.[16,17,24] PIN1 also cooperates with oncogenic KRAS in driving cellular transformation in pancreatic ductal adenocarcinoma (PDAC) and is required for PDAC cell viability.[21] Given that ICC is driven by mutant KRAS and active JNK,[4,5,8] and that a proportion of invasive ductal carcinoma breast cancer and PDAC share an inflammatory origin with ICC,[8,25,26] an interesting question is whether PIN1 plays a role in ICC. However, because genetic and/or genomic studies to date have rarely found mutations and amplifications of the PIN1 gene,[24] the molecular mechanisms underlying

View this article online at wileyonlinelibrary.com.
DOI 10.1002/hep.31983

Potential conflict of interest: Nothing to report.

ARTICLE INFORMATION:

From the [1]Leeds Institute of Medical Research at St. James', Faculty of Medicine and Health, University of Leeds, St. James' University Hospital, Leeds, United Kingdom; [2]Institute of Hepatology, Foundation for Liver Research and Birkbeck University of London, London, United Kingdom; [3]Center for Genome Engineering and Maintenance, Department of Life Sciences, College of Health, Medicine and Life Sciences, Brunel University London, Uxbridge, United Kingdom; [4]Department of Surgery and Cancer, Imperial College, London, United Kingdom; [5]Department of Infectious Disease, Imperial College, London, United Kingdom; [6]Department of Medical Physiology, Texas A&M University, Bryan, TX; [7]Division of Gastroenterology, Department of Medicine, Richard L. Roudebush VA Medical Center, Indiana University, Indianapolis, IN; [8]Cancer Research UK Cambridge Institute, University of Cambridge, Cambridge, United Kingdom; [9]Section of Gastroenterology, Ralph H. Johnson Veterans Affairs Medical Center, Charleston, SC; [10]Division of Gastroenterology and Hepatology, Department of Medicine, Medical University of South Carolina, Charleston, SC; [11]Department of Physiology, Faculty of Medicine and Nursing, University of Basque Country UPV/EHU, Leioa, Spain; [12]Institute of Biosciences and Applications, National Center for Scientific Research, Athens, Greece; [13]Department of Biochemistry and Biomedicine, School of Life Sciences, University of Sussex, Brighton, United Kingdom.

ADDRESS CORRESPONDENCE AND REPRINT REQUESTS TO:

Salvatore Papa, Ph.D.
St. James' University Hospital
Beckett Street, Wellcome Trust Brenner Building, 6.14
Leeds LS9 7TF, United Kingdom
E-mail: s.papa@leeds.ac.uk
Tel.: +44-113-343-9038

PIN1 overexpression need to be understood at the cell signaling level.

Here we demonstrate that the constitutive activation of JNK leads to elevated levels of PIN1 expression, thus promoting ICC cell proliferation. We show that JNK proteins directly interact with and phosphorylate PIN1 at Ser115. The phosphorylation of PIN1 at this specific residue directly causes the increase in intracellular PIN1 levels by preventing its mono-ubiquitination at Lys117, and, consequently, inhibiting its proteasomal degradation. We also show the potential application of PIN1 inhibition using all-trans retinoic acid (ATRA)[27] for ICC therapy.

Materials and Methods

TISSUE MICROARRAYS AND IMMUNOHISTOCHEMISTRY

Formalin fixed paraffin-embedded human ICC used in tissue microarrays (TMAs) were purchased from Pantomics (tissue block LVC1261), consisting of 42 cases, 126 cores, and one normal adjacent nontumor liver tissue core paired with two tumor tissue cores from each patient. Immunohistochemistry staining of sequential sections was carried out using a two-step protocol. After antigen retrieval, each TMA slide, consisting of serial tissue cuts, was incubated with validated anti-human PIN1 antibody (1:50; H123; Santa Cruz Biotechnology, Inc., Dallas, TX)[28] and anti-human phospho(p)-JNK (1:50; 9251; Cell Signaling Technology).[29,30] The quantification of PIN1 and phosphorylated JNK (p-JNK) staining was evaluated by randomly choosing five non-overlapping fields at ×40 for each core and quantified by counting the number of PIN1(+) or p-JNK(+) biliary epithelial cells/field and dividing by the total number of biliary epithelial cells per field.

XENOGRAFT TUMOR MODELS

For xenograft experiments, 3×10^6 CCLP1 parental or nonspecific short hairpin RNA (shNS)–expressing, JNK1/2 short hairpin RNA (shJNK1/2)–expressing, PIN1 short hairpin RNA (shPIN1)–expressing cells were injected subcutaneously into dorsal regions of 8-week-old female NOD/SCID (strain 394, Charles River) immunodeficient mice. Body weight and tumor sizes were recorded over time by a caliper, and tumor volumes were calculated using the formula $L \times W^2 \times 0.52$, where L and W represent the length and width, respectively. For ATRA treatment, 2 weeks later mice injected with CCLP1 parental cells were randomly selected to receive ATRA or control (placebo) treatment using time-release (over 21 days) drug pellets. For implantation, placebo or 10 mg of ATRA-releasing pellets (Innovative Research of America, Sarasota, FL) were implanted subcutaneously in the flank of tumor-bearing NOD/SCID mice. At sacrifice, the tumors were recovered, photographed, and the wet weight of each tumor was recorded. Each tumor was snap-frozen for further analysis. All experiments were carried out with approval from the UK Home Office Authority (PPL70/8448; PEA0105B1).[31]

STATISTICAL ANALYSIS

Statistical analyses were performed with Prism 9.0 (GraphPad Software). For two pairwise comparisons, two-tailed Student *t* tests were performed. One-way ANOVA was performed to determine differences between each group when more than two conditions were present. A two-way ANOVA test was used to test the effect of two independent variables on a dependent variable. Error bars represent the SEM. A value of $P < 0.05$ was considered significant.

Additional methods are provided as Supporting Material.

Results

JNK ACTIVITY CORRELATES WITH PIN1 EXPRESSION AND REGULATES ITS PROTEIN LEVELS IN CHOLANGIOCARCINOMA

As RAS mutations are a key event in cholangiocarcinogenesis,[4-7] and both PIN1 and JNK activation were previously identified as downstream targets of oncogenic RAS,[9-11,16,20] we investigated a possible relationship between PIN1 and JNK signaling in ICC. First, we analyzed the expression levels of PIN1 and phospho-JNK (p-JNK; a proxy for active JNK) in consecutive sections of ICC TMA by immunohistochemistry using antibodies of anti-PIN1[28] or anti-p-JNK,[29] which detect phosphorylated JNK1 and JNK2, two major JNK kinases. We found that,

compared with adjacent nontumor biliary cells, an increased percentage of ICC epithelial cells expressed PIN1 (18.64 vs. 41.25) and p-JNK (6.19 vs. 20.13), the levels of which positively correlated each other (Fig. 1A,B and Supporting Fig. S1A). Using western blot (WB), we then evaluated the expression of PIN1 and p-JNK in ICC-derived cell lines (CCLP1, HuCCT1, and SG231) and observed higher levels of both PIN1 and p-JNK in all three ICC cell lines when compared with primary normal intrahepatic biliary epithelial cells (Fig. 1C). Moreover, analysis of JNK activation by *in vitro* kinase assays showed considerable increase of the kinase activities of JNK1 and JNK2 in ICC cells compared with nontumoral immortalized human H69 cholangiocytes,[32] whereas the overall PIN1 protein levels were similar in ICC and H69 cells (Fig. 1D), suggesting a potential JNK-PIN1 pathway that is specific to ICC.

Next, we knocked down the expression of JNK proteins in ICC cells using short hairpin RNA (shRNA) lentiviruses targeting both JNK1 and JNK2 (shJNK1/2), and analyzed PIN1 expression levels. As controls, we used lentiviruses expressing shNS.[29] Efficient knockdown was verified by WB (Fig. 1E). Knockdown of JNK1/2 resulted in a marked reduction of PIN1 protein levels (Fig. 1E) with no significant effect on PIN1 mRNA levels (Fig. 1F), suggesting that JNK proteins regulate PIN1 at the post-transcriptional level. Similar results were obtained in ICC cells depleted of either JNK1 or JNK2 (Supporting Fig. S1B,C). Intriguingly, reduced PIN1 protein levels were not observed in JNK1/2-silenced H69 cells (Fig. 1E). This indicates that the effect of JNK on PIN1 expression is specific to ICC cells, in which JNK is constitutively active (see Fig. 1C,D). Indeed, a decrease in PIN1 protein levels was observed when we treated ICC cells with the JNK inhibitor SP600125[33] (Fig. 1G), which specifically blocked phosphorylation/activity of JNK1/2 without affecting phosphorylation/activity levels of other related MAPK proteins (ERK and p38).[9] Remarkably, no significant differences in phosphorylation/activity levels of JNK were observed when we knocked down PIN1 expression in ICC cells using shPIN1 (Supporting Fig. S1D), which is consistent with the hypothesis that JNK proteins function upstream of PIN1. Moreover, WB of lysates from CCLP1 cells infected with a lentivirus expressing a constitutively active form of JNK1 ($JNK1^{CA}$)[30] revealed that expression levels of endogenous PIN1 were increased compared with control cells (Fig. 1H), suggesting a role for JNK activity in up-regulating PIN1 protein levels.

PIN1 FUNCTIONALLY MIMICS JNK ACTIVATION IN CHOLANGIOCARCINOMA CELLS

Because JNK activity positively regulates PIN1 protein levels (Fig. 1E,G,H and Supporting Fig. S1B) and its inhibition impairs ICC cell proliferation,[8] we investigated whether this was the case for PIN1. Compared with control silencing, knockdown of PIN1 significantly attenuated the growth rate and reduced the colony-forming ability of ICC cells to the same extent as JNK1/2 knockdown (Fig. 2A-D and Supporting Fig. S2A-C). The growth defect of PIN1-depleted cells was specific to the lack of PIN1, as reconstituted expression of shRNA-resistant wild-type (WT) PIN1 (rPIN1 WT) in these cells reversed this defect (Supporting Fig. S2D). The effects of knockdown of either PIN1 or JNK1/2 were also confirmed by decreased cell mass accumulation (Supporting Fig. S2E-G). Notably, depletion of either PIN1 or JNK1/2 had no effect on the growth rate or cell mass accumulation of H69 cells (Fig. 2A,B and Supporting Fig. S2E-G). Furthermore, we observed a significant reduction of bromodeoxyuridine incorporation in PIN1 knockdown cells with a concomitant decrease in the levels of various cell-cycle regulators (Supporting Fig. S2H,I), indicating that PIN1 depletion attenuates ICC cell proliferation. These reductions occurred in the absence of any significant induction of apoptosis, as determined by measurement of the percentage of the sub-G1 population and caspases cleavage (Supporting Fig. S2J,K). Similar results were observed in JNK1/2 knockdown cells (Supporting Fig. S2L-O). Moreover, when subcutaneously injected into NOD/SCID immunodeficient mice, CCLP1 cells with PIN1 or JNK1/2 knockdown gave rise to smaller tumors compared with those of control silencing, as revealed by measuring tumor mass and weight (Fig. 2E-H). In contrast to the effects induced by PIN1 depletion, ectopic expression of PIN1 led to a significant increase in growth rate and colony formation of ICC cells (Fig. 2I,J). These effects faithfully mimicked those of $JNK1^{CA}$ overexpression (Fig. 2K,L). Together, these results indicate

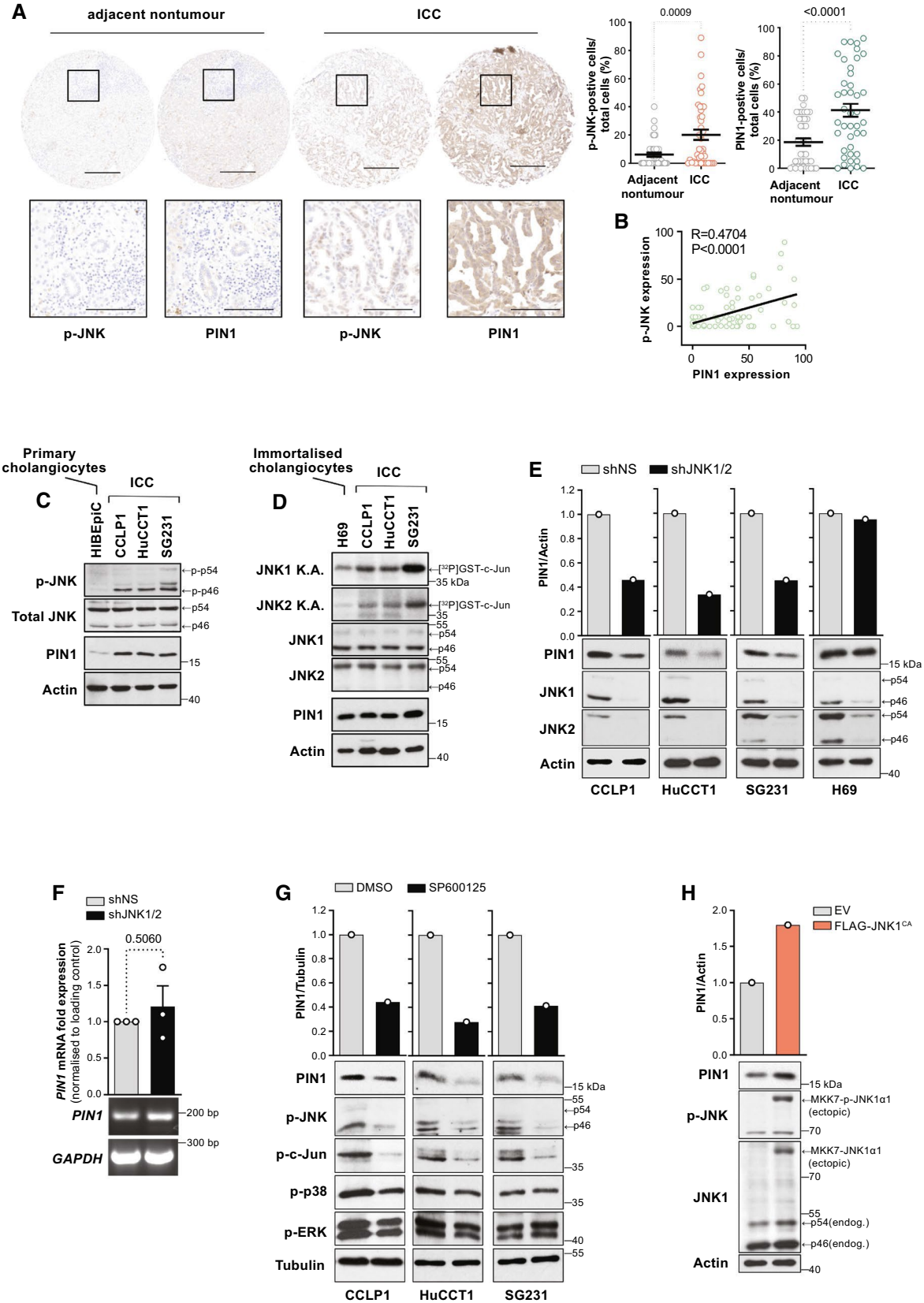
A
adjacent nontumour
ICC
p-JNK
PIN1
p-JNK
PIN1
0.0009
<0.0001
p-JNK-postive cells/ total cells (%)
PIN1-postive cells/ total cells (%)
Adjacent nontumour
ICC
B
R=0.4704
P<0.0001
p-JNK expression
PIN1 expression
Primary cholangiocytes
ICC
C
HIBEpiC
CCLP1
HuCCT1
SG231
p-JNK
Total JNK
PIN1
Actin
p-p54
p-p46
p54
p46
Immortalised cholangiocytes
ICC
D
H69
CCLP1
HuCCT1
SG231
JNK1 K.A.
JNK2 K.A.
JNK1
JNK2
PIN1
Actin
[32P]GST-c-Jun
35 kDa
E
shNS
shJNK1/2
PIN1/Actin
PIN1
JNK1
JNK2
Actin
15 kDa
CCLP1
HuCCT1
SG231
H69
F
shNS
shJNK1/2
0.5060
PIN1 mRNA fold expression (normalised to loading control)
PIN1
GAPDH
200 bp
300 bp
G
DMSO
SP600125
PIN1/Tubulin
PIN1
p-JNK
p-c-Jun
p-p38
p-ERK
Tubulin
15 kDa
CCLP1
HuCCT1
SG231
H
EV
FLAG-JNK1CA
PIN1/Actin
PIN1
p-JNK
JNK1
Actin
15 kDa
MKK7-p-JNK1α1 (ectopic)
MKK7-JNK1α1 (ectopic)
p54(endog.)
p46(endog.)

FIG. 1. Active JNK positively correlates and regulates PIN1 levels in human ICC. (A) Immunohistochemistry on serial sections of 42 paired nontumor adjacent (left panels) and ICC tissue (right panels) stained for p-JNK and PIN1. Dot plots graphs indicate the percentage of biliary cells positively stained for p-JNK and PIN1 in nontumor and ICC tissue (n = 42 per group). Data shown in the ICC group are the average results of duplicate samples. Data are presented as mean ± SEM; circles represent individual data points. *P* value was determined by Wilcoxon matched-pairs signed-rank test. Photomicrographs: scale bars = 300 μm (top) and 100 μm (bottom); magnification = ×10 (top) and ×40 (bottom). (B) Scatterplots showing the positive correlation between p-JNK and PIN1 protein expression in nontumor adjacent and ICC tissue. Pearson's coefficient tests were performed to assess statistical significance. (C) WB analyses detecting p-JNK and PIN1 in lysates of normal HIBEpiC and ICC-derived cell lines (CCLP1, HuCCT1, and SG231). Actin and total JNK were used as loading control. Arrows denote the expression levels of spliced variants p46 and p54 of JNK1 and JNK2. (D) WB and kinase assay analyses detecting PIN1 expression and JNK1 and JNK2 kinase activities in indicated ICC cell lines and nontumoral human immortalized cholangiocytes (H69).[32] Actin and total JNK1 and JNK2 protein levels were used as loading control. (E) WBs showing a reduction of PIN1 levels in indicated ICC cell lines but not in H69 cells infected with lentiviruses expressing shJNK1/2 compared with control shNS. WBs (bottom panels) showing the JNK1/2 knockdown efficiency. The bar graphs represent the quantification of the relative PIN1 levels normalized to actin. (F) Bottom: Gel of PIN1 mRNA levels, as detected by real-time PCR, in CCLP1-expressing shJNK1/2 and control shNS. Top: Graph showing quantification of the data presented as mean ± SEM; circles represent individual data points. GAPDH, control. *P* value was determined by the Student *t* test. (G) WB analyses showing a reduction of PIN1 levels in indicated ICC cell lines treated with 10 μM JNK inhibitor SP600125 compared with vehicle (DMSO)–treated control. Detection of p-JNK, p-c-Jun, p-p38, and p-ERK is shown to demonstrate effective inhibition of specific JNK kinase activity. Tubulin, control. The bar graphs represent the quantification of the relative PIN1 levels normalized to tubulin. (H) WB analyses showing increased expression of PIN1 in CCLP1 cells infected with lentiviruses expressing FLAG-tagged constitutive active JNK1 (FLAG-JNK1^{CA}) compared with EV. Actin, control. The bar graphs represent the quantification of the relative PIN1 levels normalized to actin. Results are representative of at least three independent experiments. Abbreviations: GAPDH, glyceraldehyde 3-phosphate dehydrogenase; HIBEpiC, human primary cholangiocytes; K.A., kinase assay; p-ERK, phosphorylated extracellular signal-regulated kinase.

that PIN1 promotes ICC cell proliferation both *in vitro* and *in vivo* to a similar degree as JNK activation and suggest that JNK inhibition may impair ICC cell proliferation by lowering PIN1 levels.

JNK INHIBITION DECREASES PIN1 LEVELS BY PROMOTING ITS MONOUBIQUITIN-PROTEASOME DEGRADATION

The observation that JNK1/2 knockdown results in a decrease in PIN1 protein levels without affecting the levels of its mRNA (Fig. 1E,F and Supporting Fig. S1B,C) led us to examine whether JNK1/2 regulated PIN1 protein stability. For this purpose, we evaluated the half-life of PIN1 by performing pulse-chase assays in the presence of cycloheximide (CHX), which blocks protein synthesis. Depletion of JNK1/2 or chemical inhibition of JNK activity resulted in a decrease in the half-life of endogenous PIN1 in CCLP1 cells (Fig. 3A,B). Conversely, co-expression of JNK1^{CA} but not a catalytically nonactive JNK1 protein resulted in an increase of the half-life of PIN1 in HEK293T cells (Supporting Fig. S3A,B). These findings indicate that active JNK1/2 up-regulate PIN1 levels by enhancing its protein stability.

As PIN1 has been reported to be degraded through the ubiquitin-proteasome system,[34-36] we examined whether JNK proteins elicit their effects on PIN1 stability through inactivation of the ubiquitin-proteasome system.[37] Treatment of JNK1/2-depleted ICC cells with the proteasome inhibitor MG132 was sufficient to completely revert the decrease in PIN1 protein levels in these cells (Fig. 3C), indicating that proteasome mediates the effects of JNK1/2 depletion on PIN1 levels. Similar results were obtained when we added MG132 to ICC cells pretreated with SP600125 to inhibit JNK activity (Fig. 3D). We then asked whether JNK could affect PIN1 ubiquitination, a key post-translational modification required for proteasomal degradation. FLAG-tagged PIN1 and His-tagged ubiquitin were co-expressed in HEK293T cells with or without HA-tagged JNK1^{CA}, and the ubiquitination status of PIN1 was assessed by combined Ni-NTA pull-down (PD) and WB analyses. Expression of JNK1^{CA} prevented the appearance of a single band corresponding in molecular weight to the mono-ubiquitinated form of PIN1 (Supporting Fig. S3C). Such an effect was also confirmed by co-immunoprecipitation (IP) analyses (Supporting Fig. S3D). Similar results were obtained when a mutant form of ubiquitin (UbK0), which allows only mono-ubiquitination due to the lack of lysine residues,[38] was used instead of WT ubiquitin (Supporting Fig. S3E). This confirms that PIN1 is subject to mono-ubiquitination, which is inhibited by

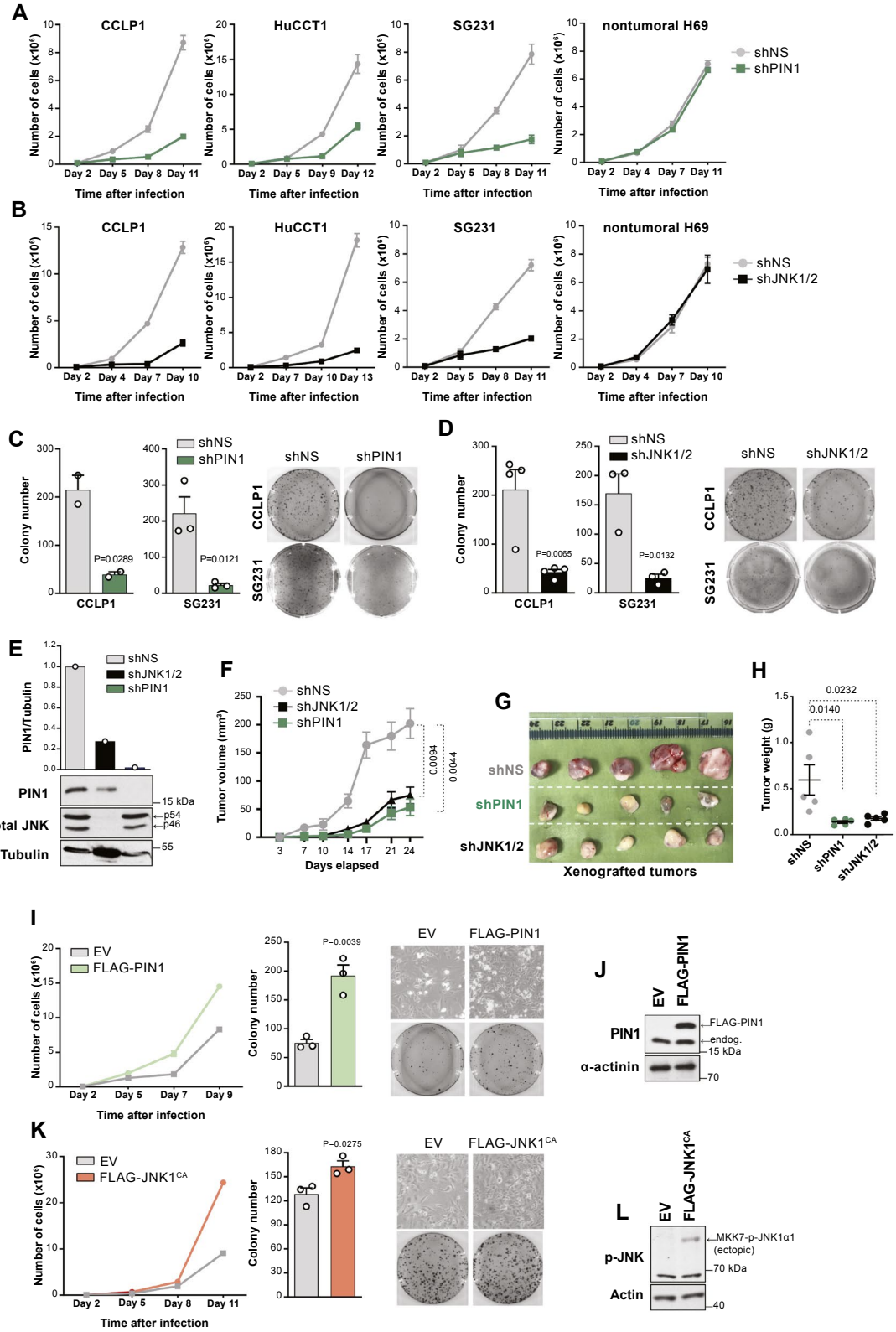
A
CCLP1
HuCCT1
SG231
nontumoral H69
Number of cells (x10⁶)
Time after infection
shNS
shPIN1
B
shJNK1/2
C
Colony number
P=0.0289
P=0.0121
D
P=0.0065
P=0.0132
E
PIN1/Tubulin
PIN1
Total JNK
Tubulin
15 kDa
p54
p46
55
F
Tumor volume (mm³)
Days elapsed
0.0094
0.0044
G
Xenografted tumors
H
Tumor weight (g)
0.0232
0.0140
I
EV
FLAG-PIN1
P=0.0039
J
FLAG-PIN1
endog.
α-actinin
70
K
FLAG-JNK1CA
P=0.0275
L
MKK7-p-JNK1α1 (ectopic)
p-JNK
70 kDa
Actin
40

FIG. 2. JNK activity and PIN1 expression are similarly required for ICC cell growth both *in vitro* and *in vivo*. (A,B) Growth curves of CCLP1 (n = 6), HuCCT1 (n = 6), SG231 (n = 3), and nontumoral H69 cholangiocytes (n = 3) stably expressing PIN1, JNK1/2, or shNS. Data are shown as mean ± SEM and are representative of three independent cultures. (C,D) Anchorage-independent colony formation of CCLP1 and SG231 cells stably expressing shPIN1, shJNK1/2, or shNS. Representative images show overall view of colony growth after 3 weeks. Data shown are mean ± SEM of three independent cultures, and circles represent individual data points. *P* values were calculated by Student *t* test. (E) WBs showing PIN1 and JNK1/2 protein levels in lysates from CCLP1 cells stable-expressing shNS, shJNK1/2, or shPIN1 used in xenograft experiments (injected cells). Tubulin and total JNK levels were analyzed with appropriate antibodies as controls. The bar graphs represent the quantification of the relative PIN1 levels normalized to tubulin. (F) Curves of tumor volume plotted over time following inoculation of CCLP1 cells described in (E). *P* values were calculated using the two-way ANOVA test. (G) Shown are sizes of tumors developed in mice 24 days following inoculation with CCLP1 cells as described in (E). (H) Tumor weight of explanted tumors at day 24 following post-inoculation. *P* values were calculated from one-way ordinary ANOVA test adjusted with Tukey's multiple comparison tests. (I,K) Growth curves and anchorage-independent colony formation of CCLP1 ectopically expressing either FLAG-PIN1 (n = 3) (I) or FLAG-JNK1^{CA} (n = 3) (K) compared with EV (n = 3). Shown are representative light microscopy images of cultured cells (days 7 or 8 after complementary DNA expression) and overall view of colony growth after 3 weeks. Data shown are mean ± SEM of three independent cultures; circles represent individual data points. *P* values were calculated by Student t test. (J,L) WBs showing the ectopic or endogenous (endog.) levels of PIN1 and p-JNK in CCLP1 stably expressing FLAG-PIN1 (J) or FLAG-JNK1^{CA} (L).

JNK1^{CA} expression. Such inhibition was not observed when we co-expressed the catalytically nonactive JNK1 protein (Supporting Fig. S3F), suggesting that JNK kinase activity is required for preventing PIN1 mono-ubiquitination. Importantly, the inhibitory effect of JNK on PIN1 mono-ubiquitination was confirmed in ICC cells, as accumulation of endogenous mono-ubiquitinated PIN1 was observed in JNK1/2-depleted CCLP1 cells (Fig. 3E). Thus, the constitutive activation of JNK in ICC cells leads to high levels of PIN1 by preventing its mono-ubiquitination and degradation.

ACTIVE JNK PROTEINS INTERACT WITH AND PHOSPHORYLATE PIN1 AT Ser115

To gain insight into the mechanism by which JNK proteins stabilize PIN1, we co-expressed HA-tagged PIN1 in HEK293T cells with FLAG-tagged JNK1^{CA}, FLAG-tagged JNK2^{CA} or empty vector, and investigated protein associations by combined IP and WB analyses. Both FLAG-tagged JNK1^{CA} and FLAG-tagged JNK2^{CA} specifically bound to HA-PIN1 (Supporting Fig. S4A). Furthermore, *in vitro* kinase assays revealed that both active JNK1 and JNK2 efficiently phosphorylated recombinant glutathione S-transferase (GST)–fused PIN1, but not GST alone (Fig. 4A). As JNK1 and JNK2 shared common function with respect to their interaction with PIN1 and its phosphorylation, we focused our attention on JNK1 in further analyses. First, the interaction between PIN1 and active JNK1 was confirmed at the endogenous levels. Anti-active JNK1 antibodies[29,30] co-immunoprecipitated PIN1 from parental cells, but not from ICC cells depleted of PIN1 (WB:PIN1; Fig. 4B). JNK1 was immunoprecipitated at comparable levels in both parental cells and PIN1-depleted cells and was not co-precipitated by isotype-matched control antibodies (WB:JNK1; Fig. 4B). We then verified that PIN1 was phosphorylated by JNK1 in *in vivo* cells. PIN1 co-expressed with JNK1^{CA}, but not with the catalytically nonactive JNK1 protein, was highly phosphorylated in HEK293T cells, as shown by a marked band shift of PIN1 on Phos-tag polyacrylamide gel electrophoresis.[39] This shifted band disappeared when cell lysates were treated with the calf intestinal alkaline phosphatase (CIP) (Supporting Fig. S4B), confirming that the shifted band of PIN1 was a consequence of phosphorylation by active JNK1. Importantly, phosphorylation of endogenous PIN1 by JNK was confirmed in ICC cells, as the PIN1-shifted band disappeared in JNK1/2-depleted or SP600125-treated CCLP1 cells on Phos-tag immunoblots (Fig. 4C), indicating that PIN1 is indeed phosphorylated by JNK proteins in ICC cells.

To test whether JNK could directly phosphorylate PIN1, we performed *in vitro* kinase assays and found that recombinant active JNK1 efficiently phosphorylated purified His-PIN1 (Fig. 4D). Accordingly, *in vitro* pull-down analyses revealed direct interaction between active JNK1 and PIN1 (Fig. 4E). Altogether, these data indicate that PIN1 is a direct substrate of JNK1 kinase. In support of this notion, a single phosphorylation site (Ser115) was detected in PIN1 by mass spectrometry (Supporting Fig. S4C-F).

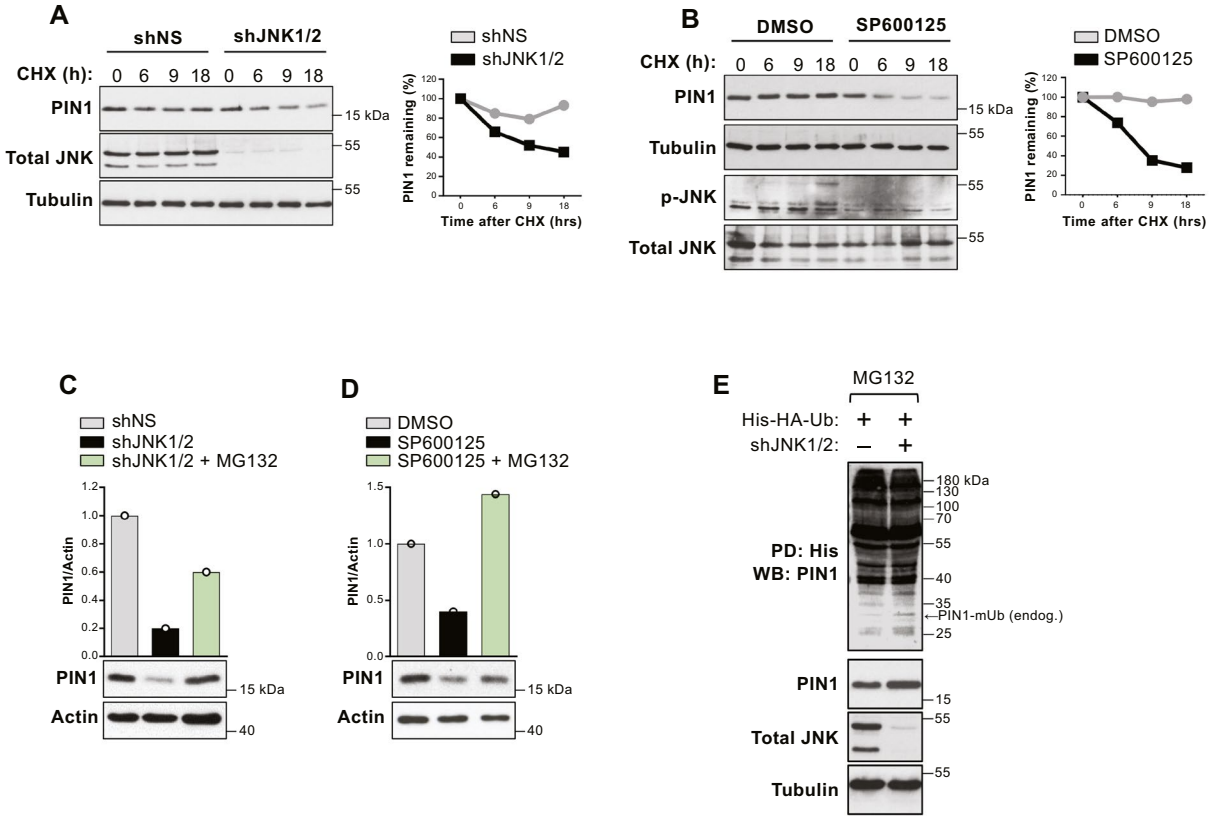

FIG. 3. Constitutive activation of JNK stabilizes PIN1 protein by preventing its mono-ubiquitination and degradation. Results shown are representative of at least three independent experiments. (A) Analysis of PIN1 protein stability by pulse-chase experiments in JNK1/2-depleted CCLP1 cells. WB analyses of PIN1 levels in shJNK1/2-expressing and shNS-expressing CCLP1 cells treated with CHX for the indicated times. Quantification of PIN1 levels relative to tubulin is shown on the right panel. (B) WB analyses of PIN1 levels in CCLP1 cells pretreated with SP600125 (10 μM) for 24 hours, followed by CHX treatment for the indicated times. Quantification of PIN1 levels relative to tubulin is shown on the right panel. (C) WBs showing PIN1 abundance in JNK1/2-depleted CCLP1 cells treated with either 10 μM MG132 or DMSO (control) for 24 hours. The bar graphs represent the quantification of the relative PIN1 levels normalized to actin. shNS-expressing CCLP1 cells are used as control. (D) WBs showing PIN1 abundance in CCLP1 treated with SP600125 (10 μM) for 24 hours followed by co-treatment of SP600125 with either 10 μM MG132 or DMSO (control) for an additional 24 hours. The bar graphs represent the quantification of the relative PIN1 levels normalized to actin. Parental CCLP1 cells treated with DMSO alone are used as control. (E) *In vivo* ubiquitination assays showing accumulation of endogenous mono-ubiquitinated PIN1 in JNK1/2-depleted CCLP1 cells overexpressing His-HA-tagged ubiquitin, in the presence of MG132. Ubiquitinated proteins were pulled down with Ni-NTA beads and analyzed by WBs using anti-PIN1 antibody. The arrow indicates the mono-ubiquitinated PIN1 (PIN1-mUb) band.

Sequence alignment analysis of PIN1 revealed that Ser115 is conserved among different species and located within the consensus phosphorylation motif for JNKs (^{115}SA^{116})[40] (Supporting Fig. S4G). To confirm Ser115 as the specific JNK1 phosphorylation site on PIN1, a non-phosphorylatable alanine PIN1 mutant (S115A) was generated and used as a substrate for JNK1 in kinase assays. As controls, we individually mutated Ser114, a nearby JNK consensus phosphorylation site (^{114}SS^{115}), and Ser138, a residue known to be phosphorylated by the JNK-related kinase mixed-lineage kinase 3,[41] into alanines (S114A and S138A). PIN1-S115A mutant, but not WT PIN1, PIN1-S114A or PIN1-S138A mutant, was resistant to phosphorylation by JNK1 *in vitro* (Fig. 4F). This result was confirmed in ICC cells expressing endogenous active JNK and in HEK293T cells expressing exogenous constitutively active JNK1 by Phos-tag immunoblots (Fig. 4G and Supporting Fig. S4H). Taken together, these results indicate that JNK1 directly phosphorylates PIN1 at Ser115 both *in vitro* and in *in vivo* cells.

PHOSPHORYLATION OF PIN1 AT Ser115 PREVENTS ITS MONO-UBIQUITINATION AND DEGRADATION

To directly test the role of Ser115 phosphorylation in the control of PIN1 protein stability, we generated CCLP1 cells stably expressing FLAG-PIN1-WT, FLAG-PIN1-S114A, FLAG-PIN1-S115A, or FLAG-PIN1-S138A mutant and assessed the half-life of PIN1 mutant proteins in these cells, which have endogenous active JNK (Fig. 1C,D). Endogenous active JNK failed to prolong the half-life of the PIN1-S115A mutant, but not of PIN1-WT, PIN1-S114A, or PIN1-S138A mutant (Fig. 5A), implying that phosphorylation of PIN1 at Ser115 is required for PIN1 protein stability. Accordingly, PIN1-S115A mutant was heavily mono-ubiquitinated in CCLP1 cells, whereas WT PIN1 was resistant to mono-ubiquitination (Fig. 5B), indicating

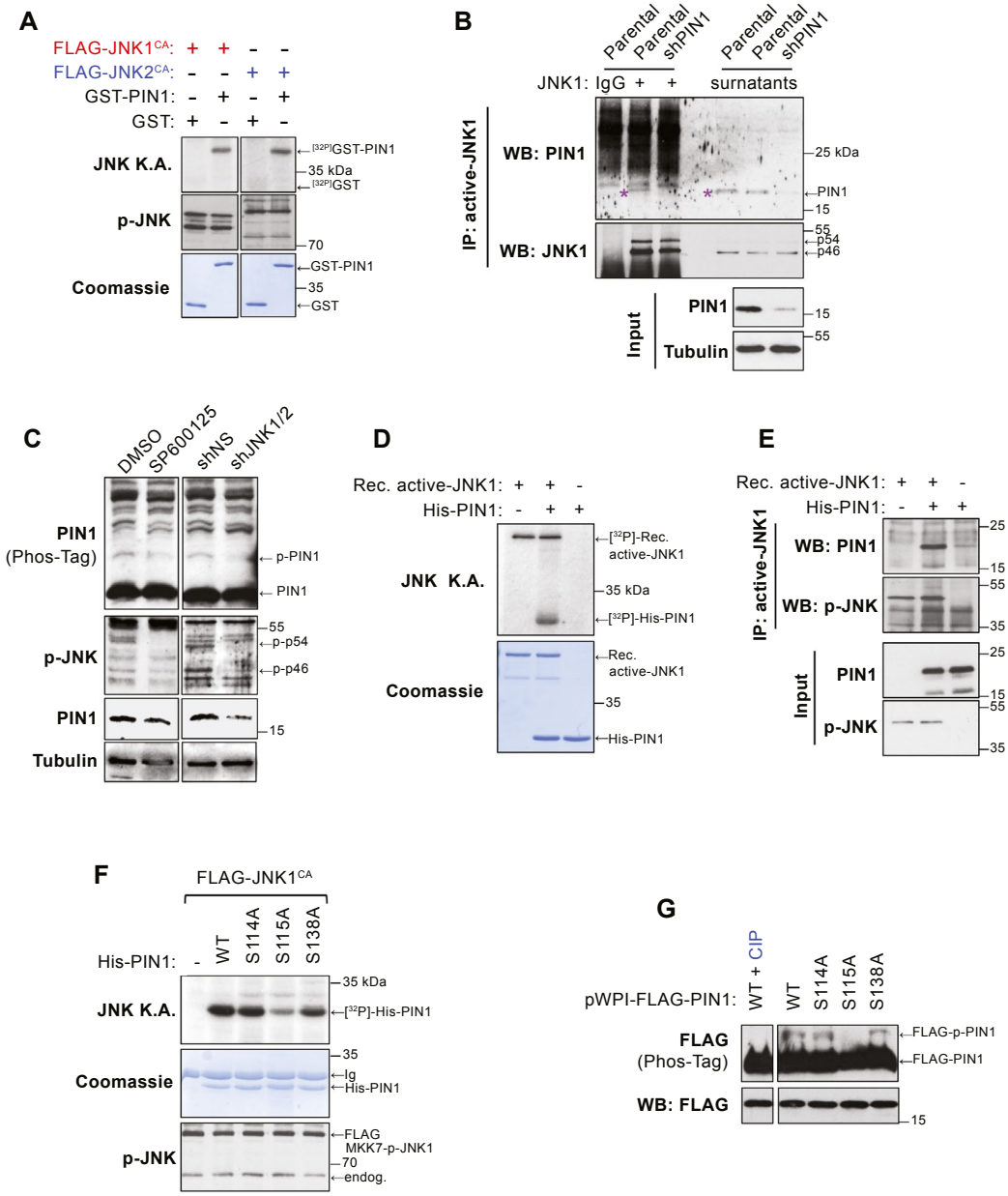

FIG. 4. JNK directly binds to and phosphorylates PIN1 at Ser115. Results shown are representative of at least three independent experiments. (A) Constitutive active JNK1 or JNK2 were immunoprecipitated from lysates of HEK293T cells expressing FLAG-tagged $JNK1^{CA}$ or FLAG-$JNK2^{CA}$, respectively, and assayed for kinase activity using recombinant GST-PIN1 or control GST proteins as substrates in the presence of (^{32}P)-γ-ATP. WB and Coomassie blue staining indicate loading controls in the bottom panels. (B) IP followed by WBs showing endogenous association of active JNK1 with PIN1 in parental CCLP1 cells. IP against IgG and lysates of PIN1-depleted (shPIN1) CCLP1 cells were used as control. The purple-colored asterisks indicate PIN1 band present in the anti-PIN1 blot. (C) Phos-tag analysis in JNK1/2-depleted or SP600125-treated CCLP1 ICC cells showing reduction of endogenous phospho(p)-PIN1 levels compared with control cells (shNS; DMSO). Tubulin, loading control. (D) *In vitro* JNK kinase assay was performed by incubating recombinant activated JNK1 with His-PIN1 as substrate. [^{32}P]-Rec. active-JNK1 denotes autophosphorylation. Coomassie staining shows the purity and size of the recombinant proteins. (E) *In vitro* PD assay showing a direct binding between purified active JNK1 and PIN1. The assay was performed by IP and WB after incubating purified recombinant activated JNK1 and His-PIN1 (IP:JNK1 and WB:PIN1). (F) Activated JNK was immunoprecipitated from lysates of HEK293T cells expressing FLAG-tagged $JNK1^{CA}$ and assayed for kinase activity using purified His-tagged PIN1-WT, PIN1-S114A, PIN1-S115A, or PIN1-S138A as substrate in the presence of (^{32}P)-γ-ATP. WB against p-JNK and Coomassie staining indicate loading controls. (G) Phos-tag analysis of PIN1 S115 phosphorylation by endogenous JNK in CCLP1 cells stably expressing PIN1-WT or the indicated PIN1 mutants. Phosphorylated PIN1 band is absent in CCLP1 cells expressing FLAG-PIN1(S115A) mutant. An aliquot of lysates from CCLP1 cells expressing FLAG-PIN1-WT was treated with CIP before electrophoresis and loaded onto the same gel on a distant lane. All of the other samples were incubated at 37°C in the presence of CIP buffer only. Bottom: Standard WBs were carried on whole-cell lysates using anti-FLAG antibody. Abbreviations: K.A., kinase assay; Rec. active-JNK1, recombinant activated JNK1.

that PIN1-S115A mutant is targeted for degradation. Similar results were observed in HEK293T cells ectopically expressing $JNK1^{CA}$ (Supporting Figs. S5A,B and S3C). Collectively, these data indicate that JNK-mediated PIN1 phosphorylation at Ser115 is essential for PIN1 protein stability. We next sought to identify the lysine residue on PIN1, which is targeted for mono-ubiquitination. As most protein ubiquitination sites tend to be exposed to the solvent,[42,43] we calculated the solvent-accessible surface area (SASA) of the 10 lysine residues (K6, K13, K46, K63, K77, K82, K95, K97, K117, and K132) in the high-resolution X-ray crystal structure of PIN1 (PDB ID:1PIN).[44] Lys117 emerged as the lysine residue with the highest solvent accessibility (Fig. 5C and Supporting Table S1), suggesting that K117 is a highly exposed residue and may therefore serve as the PIN1 ubiquitination site. Indeed, mutation of Lys117 to arginine (K117R) abolished mono-ubiquitination of PIN1 (Fig. 5D and Supporting Fig. S5C), and subsequently resulted in an increase of PIN1 half-life in *in vivo* cells (Fig. 5E and Supporting Fig. S5D). Although we cannot completely rule out by site-directed mutagenesis that other lysine residues within PIN1 could be targets for mono-ubiquitination, mutating Lys46, which has the second highest solvent accessibility, did not abrogate the ubiquitination of PIN1 (Supporting Fig. S5C). These results indicate that, most likely, Lys117 residue on PIN1 is the major site subjected to mono-ubiquitination needed for its degradation.

To gain insights into the structural basis of Ser115 phosphorylation-mediated inhibition of PIN1 mono-ubiquitination, we performed atomistic molecular dynamics (MD) simulations in explicit solvent of unphosphorylated Ser115 (S115) and phosphorylated Ser115 (p-S115) PIN1 (Supporting Fig. S5E; see also Supporting Methods). Five independent MD simulations of 100 ns were carried out for each Ser115 state, starting from the crystallographic coordinates of PIN1 resolved at 1.35 Å.[44] Comparison of the atomic RMS deviations (RMSDs) from the starting structure revealed that, although both unphosphorylated and phosphorylated PIN1 displayed low deviations with respect to the X-ray structure, phosphorylated PIN1 showed higher deviations compared with the unphosphorylated PIN1 (Supporting Fig. S5F,G). Consistent with the RMSD results, analyses of the atomic RMS fluctuations revealed a significant increase in the flexibility of residues 115-117 upon phosphorylation of Ser115 (Supporting Fig. S5H). Taken together, our simulations suggest that phosphorylation at Ser115 induces significant local changes in the dynamics of PIN1. Interestingly, analyses of the SASA value for the 10 lysine residues of PIN1 throughout the MD simulations revealed a significant decrease in the solvent accessibility of Lys117 upon phosphorylation of Ser115 (Supporting Fig. S5I). All other lysine residues displayed no significant differences in the average SASA values between the unphosphorylated and phosphorylated PIN1 systems (Fig. 5F). Representative snapshots from one of the

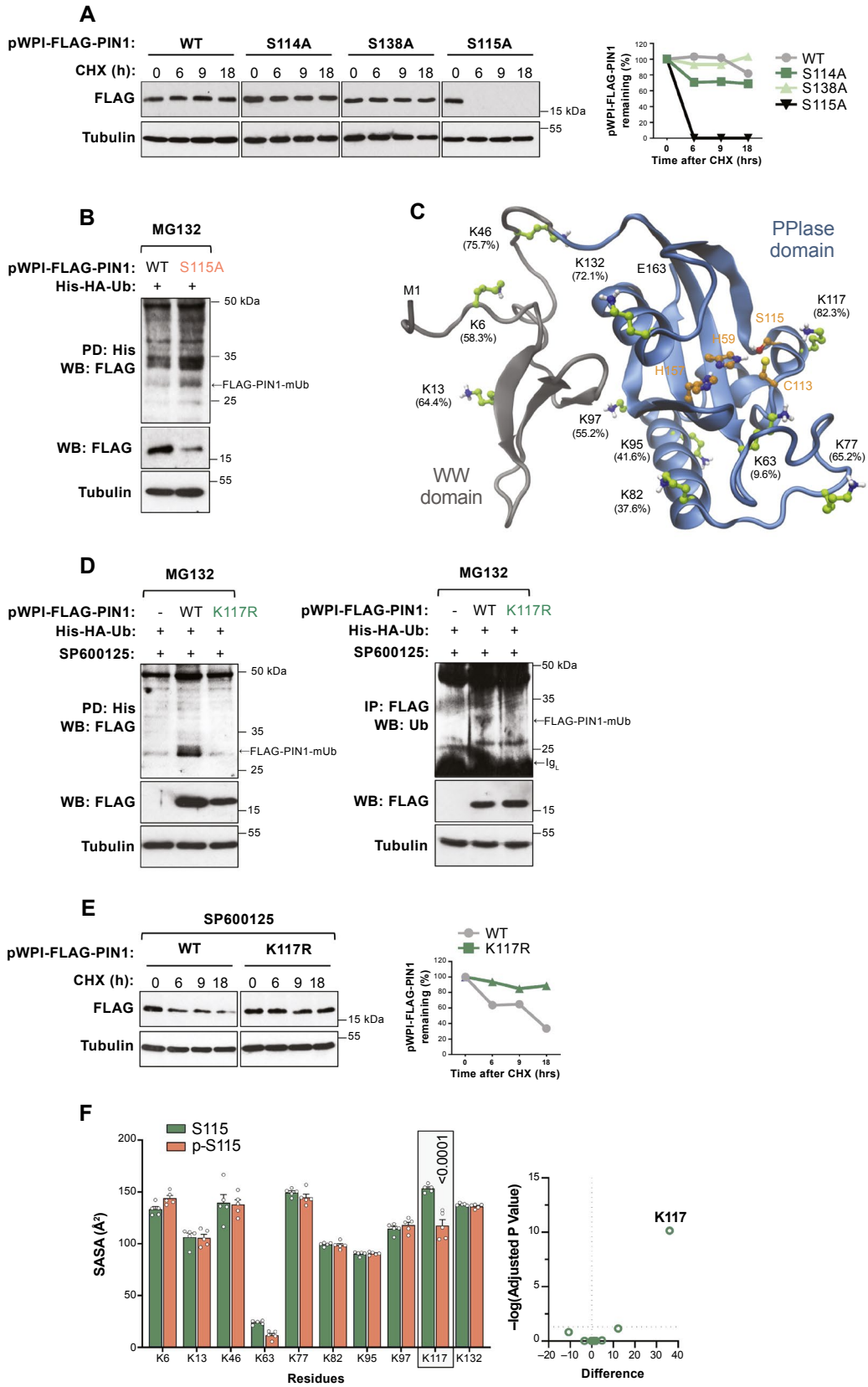
A
pWPI-FLAG-PIN1:
WT
S114A
S138A
S115A
CHX (h):
0 6 9 18
FLAG
Tubulin
15 kDa
55
pWPI-FLAG-PIN1 remaining (%)
Time after CHX (hrs)
WT
S114A
S138A
S115A
B
MG132
pWPI-FLAG-PIN1:
WT S115A
His-HA-Ub:
+ +
PD: His
WB: FLAG
50 kDa
35
FLAG-PIN1-mUb
25
WB: FLAG
15
Tubulin
55
C
PPIase domain
WW domain
K46 (75.7%)
K132 (72.1%)
E163
M1
K6 (58.3%)
K117 (82.3%)
S115
H59
H157
C113
K13 (64.4%)
K97 (55.2%)
K95 (41.6%)
K63 (9.6%)
K77 (65.2%)
K82 (37.6%)
D
MG132
pWPI-FLAG-PIN1:
- WT K117R
His-HA-Ub:
+ + +
SP600125:
+ + +
PD: His
WB: FLAG
IP: FLAG
WB: Ub
50 kDa
35
FLAG-PIN1-mUb
25
IgL
WB: FLAG
15
Tubulin
55
E
SP600125
pWPI-FLAG-PIN1:
WT
K117R
CHX (h):
0 6 9 18
FLAG
Tubulin
15 kDa
55
pWPI-FLAG-PIN1 remaining (%)
Time after CHX (hrs)
F
S115
p-S115
SASA (Å²)
<0.0001
K6 K13 K46 K63 K77 K82 K95 K97 K117 K132
Residues
–log(Adjusted P Value)
K117
Difference

FIG. 5. JNK-mediated PIN1 Ser115 phosphorylation prevents its mono-ubiquitination at Lys117. Results shown are representative of at least three independent experiments. (A) Analysis of PIN1 WT and PIN1 mutant proteins stability by pulse-chase experiments. CCLP1 cells overexpressing FLAG-tagged PIN1-WT or PIN1 mutants (S114A, S115A, and S138A) were treated with CHX for the indicated times, harvested, and analyzed by WBs as indicated. Quantification of FLAG-PIN1 levels relative to tubulin is shown on the right panel. (B) *In vivo* ubiquitination assays showing the level of mono-ubiquitination of PIN1-WT and PIN1-S115A mutant proteins in CCLP1 cells stably co-expressing His-HA-ubiquitin with FLAG-PIN1-WT or FLAG-PIN1-S115A, in the presence of MG132. Ubiquitinated proteins were pulled down with Ni-NTA beads and analyzed by WB using anti-FLAG antibody. (C) Ribbon representation of PIN1 color-coded by domain (gray, WW domain; blue, PPIase domain). The 10 lysine residues of the enzyme are shown with ball-and-sticks (green C, blue N, and white H atoms), and values in parentheses indicate the relative solvent accessibility of their side-chain atoms (RSA, %), as calculated from a high-resolution crystal structure of PIN1 (PDB ID: 1PIN) using NACCESS. Also shown with orange C atoms are S115, C113, and the catalytic site histidine residues H59 and H157 (O atoms are shown in red and S in yellow). (D) *In vivo* ubiquitination assay in SP600125-treated CCLP1 cells stably co-expressing His-HA-ubiquitin with FLAG-PIN1-WT or FLAG-PIN1-K117R. Left: Ubiquitinated proteins were pulled down with Ni-NTA beads and analyzed by WBs using anti-FLAG antibody. Right: IP with anti-FLAG antibody followed by WBs with anti-ubiquitin antibody. (E) Analysis of PIN1-WT and PIN1-K117R proteins stability by pulse-chase experiments. Following treatment with SP600125, CCLP1 cells overexpressing FLAG-PIN1-WT or FLAG-PIN1-K117R mutant were treated with CHX for the indicated times, harvested, and analyzed by WB as indicated. Quantification of FLAG-PIN1 levels relative to tubulin is shown on the right panel. (F) Left: Plot of the mean SASA for each lysine residue of PIN1 (side-chain atoms only), calculated from (n = 5) independent 100-ns MD simulations of the enzyme in the unphosphorylated (S115) or phosphorylated (p-S115) state of Ser115. Data in bar graph are presented as mean ± SEM; circles represent individual data points. *P* values were calculated using the multiple t-test. Right: Volcano plot showing the estimated SASA fold changes between S115 and p-S115 (x-axis) versus the $-\log_{10}$ *P* values (y-axis) for each lysine of PIN1. Dotted grid lines are shown at x = 0 (no difference) and y = $-\log_{10}(0.05)$. K117 is the only lysine showing a significant difference. Abbreviation: Ub, ubiquitin.

five simulations of phosphorylated PIN1 are shown in Supporting Fig. S5J, to illustrate the decrease in the SASA of K117 (from 165 Å to 68 Å) during the course of the simulation time. These observations suggest that PIN1 phosphorylation at Ser115 may inhibit its mono-ubiquitination by decreasing surface exposure of the Lys117 residue, and thus its accessibility, for ubiquitination.

PIN1 Ser115 PHOSPHORYLATION PROMOTES CHOLANGIOCARCINOMA PROLIFERATION

We then examined the biological significance of JNK-mediated PIN1 Ser115 phosphorylation on PIN1 function in ICC cells. ICC cells depleted of endogenous PIN1 were reconstituted with rPIN1 WT, shRNA-resistant PIN1 S115A (rPIN1 S115A) or empty vector (EV), and growth rate and colony-forming capacity of ICC cells were evaluated. Ectopic expression of rPIN1 WT and rPIN1 S115A was verified by WB (Fig. 6A). Of note, rPIN1 WT and rPIN1 S115A had comparable cellular levels that were similar to those of endogenous PIN1 in parental cells (Fig. 6A; top panel). In parallel, Phos-tag WB analyses further confirmed that S115A mutation abolishes JNK-mediated phosphorylation signal in ICC cells (Fig. 6A; see also Fig. 4C). Reconstitution with rPIN1 S115A, but not rPIN1 WT, failed to rescue the impaired growth rate and ability to grow colonies of PIN1-depleted cells (Fig. 6B,C). Moreover, expression of key positive cell-cycle regulators and transcriptional activity of NF-κB (a well-established PIN1 target and ICC cell growth marker)[20,45] were restored by reconstituted expression of rPIN1 WT, but not by that of rPIN1 S115A mutant (Fig. 6A,D). Thus, phosphorylation of PIN1 at Ser115 by active JNK is critical for promoting ICC cell proliferation.

PHARMACOLOGICAL INHIBITION OF PIN1 IMPAIRS CHOLANGIOCARCINOMA GROWTH

The prolific role of PIN1 in cancer has triggered extensive efforts to design small molecule inhibitors targeting PIN1 function.[19-24,36] One such potent inhibitor of PIN1 is ATRA, which binds to PIN1 and induces its degradation.[27,36] As the JNK-PIN1 regulatory axis sustains ICC cell proliferation, we explored whether ATRA-induced PIN1 degradation could be used as a therapeutic strategy in cholangiocarcinoma. First, we treated ICC cells with increasing concentrations of ATRA and observed that ATRA treatment resulted in a dose-dependent decrease in the growth rate of ICC cells; however, ATRA had no effect on nontumoral H69 cholangiocytes (Fig. 7A).

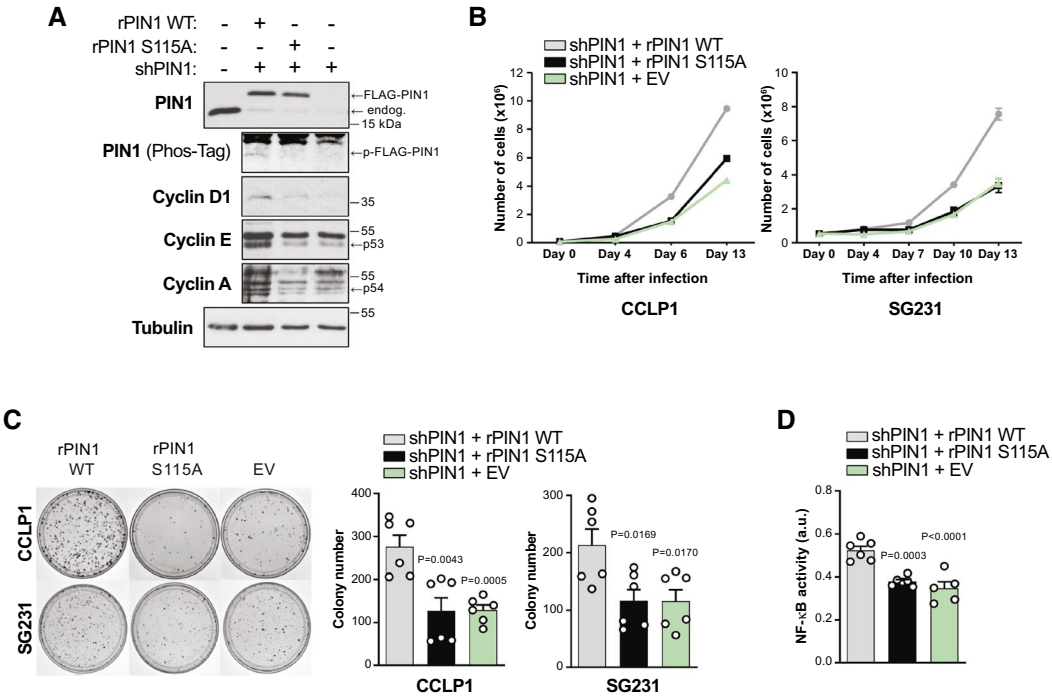

FIG. 6. PIN1 Ser115 phosphorylation promotes ICC cell growth. (A) Representative of three independent WBs showing the effect of PIN1 reconstitution in CCLP1 cells depleted of endogenous PIN1. Cells were reconstituted with complementary DNA expressing shRNA-resistant FLAG-PIN1 WT (rPIN1 WT), FLAG-PIN1 S115A (rPIN1 S115A), or EV (-). Lysates of CCLP1 parental cells (first lane) were used as control for endogenous PIN1 expression levels. Shown are Phos-tag and classic WB analyses displaying a correlation of expression between phospho(p)-PIN1 levels and cyclin D1, E, and A. Tubulin was used as loading control. (B) shPIN1-expressing CCLP1 and SG231 ICC cells were reconstituted with rPIN1 WT, rPIN1 S115A or EV, and cell growth was quantified at the indicated times. Data are presented as mean ± SEM. (C) Colony-formation assay was performed in shPIN1-expressing CCLP1 and SG231 cells reconstituted with rPIN1 WT, rPIN1 S115A, or EV. Data are presented as mean ± SEM, and circles represent individual data points. *P* values were calculated using the one-way ordinary ANOVA test adjusted with Dunnett's multiple comparison tests. (D) Transcriptional activity of NF-κB (left) and signal transducer and activator of transcription 3 (right) in shPIN1-expressing CCLP1 cells reconstituted with rPIN1 WT, rPIN1 S115A, or EV. Data are presented as mean ± SEM; circles represent individual data points. *P* values were calculated using the one-way ordinary ANOVA test adjusted with Dunnett's multiple comparison tests. Abbreviations: a.u., arbitrary units; endog., endogenous.

As expected, the decrease in the cell growth rate was associated with a dose-dependent decrease in PIN1 protein levels (Fig. 7B), confirming that ATRA prevents PIN1 accumulation in ICC cells. Notably, ATRA treatment did not affect the phosphorylation/activity levels of JNK (Fig. 7B). A dose-dependent growth inhibitory effect of ATRA was also observed in ICC cells ectopically expressing PIN1 (Fig. 7C). Next, we subcutaneously injected CCLP1 cells into NOD/SCID immunodeficient mice, and 2 weeks later we implanted either ATRA-releasing pellets or placebo pellets into the flanks of mice to assess the effects of ATRA on the ability of ICC cells to form tumors *in vivo* (Supporting Fig. S6A). After a median tumor growth period of 26 days, smaller tumors developed in ATRA-treated group compared with those in placebo-treated mice, as revealed by measuring tumor mass and tumor weight (Fig. 7D-F and Supporting Fig. S6B). WB analyses showed that PIN1 levels markedly decreased in the ATRA-treated tumors compared with those in placebo-treated tumors (Supporting Fig. S6C). Notably, expression levels of PIN1 did not correlate with those of p-JNK in tumors from ATRA-treated mice (Supporting Fig. S6C; see also Fig. 7B), suggesting a potential disruption of JNK-PIN1 regulatory axis by ATRA. These results suggest that ATRA-induced PIN1 degradation may have therapeutic potential against

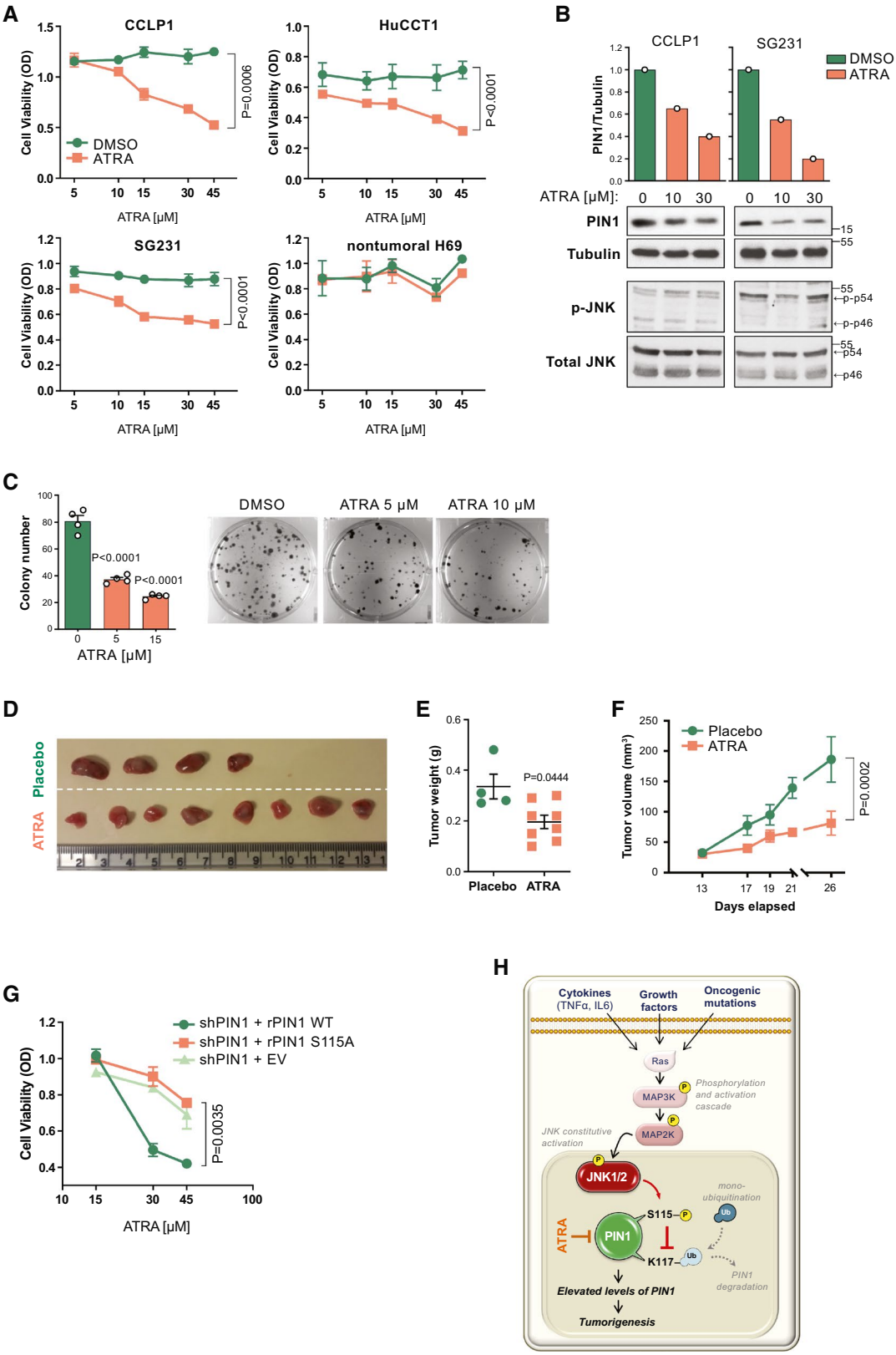
A
CCLP1
HuCCT1
SG231
nontumoral H69
Cell Viability (OD)
ATRA [μM]
DMSO
ATRA
P=0.0006
P<0.0001
P<0.0001
B
CCLP1
SG231
DMSO
ATRA
PIN1/Tubulin
ATRA [μM]: 0 10 30 0 10 30
PIN1
Tubulin
p-JNK
Total JNK
55
p-p54
p-p46
p54
p46
C
Colony number
P<0.0001
P<0.0001
ATRA [μM]
DMSO
ATRA 5 μM
ATRA 10 μM
D
Placebo
ATRA
E
Tumor weight (g)
P=0.0444
Placebo
ATRA
F
Placebo
ATRA
Tumor volume (mm³)
P=0.0002
Days elapsed
G
shPIN1 + rPIN1 WT
shPIN1 + rPIN1 S115A
shPIN1 + EV
Cell Viability (OD)
P=0.0035
ATRA [μM]
H
Cytokines (TNFα, IL6)
Growth factors
Oncogenic mutations
Ras
MAP3K
Phosphorylation and activation cascade
MAP2K
JNK constitutive activation
JNK1/2
mono-ubiquitination
S115
K117
PIN1
ATRA
PIN1 degradation
Elevated levels of PIN1
Tumorigenesis

FIG. 7. PIN1 inhibition by ATRA impairs cholangiocarcinoma growth *in vivo*. (A) Cell viability assay of CCLP1, HuCCT1, SG231 ICC cells, and nontumoral H69 cholangiocytes treated with ATRA for 72 hours and assayed with colorimetric MTT assay. Data are shown as mean ± SEM and are the combination of (n = 4) independent cultures. *P* values were calculated using the two-way ANOVA test. (B) WB and quantification analyses showing reduction of PIN1 levels, but not of p-JNK, in CCLP1 and SG231 ICC cell lines following 48 hours treatment with the indicated concentrations of ATRA. Tubulin and total-JNK were used as loading controls. (C) Anchorage-independent colony formation of CCLP1 expressing FLAG-PIN1 and treated with the indicated concentrations of ATRA. Representative images show overall view of colony growth after 3 weeks. Data are shown as mean ± SEM of four independent cultures; circles represent individual data points. *P* values were calculated using the one-way ordinary ANOVA test adjusted with Dunnett's multiple comparison tests. (D) Shown are sizes of tumors developed in nude mice inoculated with CCLP1 cells, and 13 days later implanted with ATRA-releasing (10 mg over 21 days) or placebo (control) pellets. (E) Tumor weight of explanted tumors at day 26 following ATRA or placebo treatment. *P* value was calculated using the Student *t* test. (F) Curves of tumor volume plotted over time following ATRA or placebo treatment. *P* values were calculated using the two-way ANOVA test. (G) Cell viability assay of shPIN1-expressing CCLP1 cells reconstituted with rPIN1 WT, rPIN1 S115A, or EV and treated with the indicated concentrations of ATRA for 72 hours. Data are shown as mean ± SEM and are the combination of three independent cultures. *P* values were calculated using the two-way ANOVA test. (H) Schematic illustration depicting the mechanism of action of JNK-mediated cholangiocarcinogenesis. In response to growth factors, inflammatory cytokines and oncogenic signals, cancer cells activate the JNK signaling pathway through a phosphorylation cascade that involves oncogenic RAS, MAP3K, and MAP2K. Active JNK directly binds and phosphorylates PIN1 at S115. This phosphorylation prevents PIN1 mono-ubiquitination at Lys117 (K117) and subsequent proteasomal degradation, contributing to the intracellular accumulation of PIN1 in cancer cells. The targeting of PIN1 with ATRA uncouples the JNK-PIN1 axis and impairs the JNK-mediated cholangiocarcinogenesis. Abbreviations: MTT, 3-(4,5-dimethylthiazol-2-yl)-2,5-diphenyltetrazolium bromide; P, phosphorylation; Ub, ubiquitin.

cholangiocarcinoma growth. Finally, we examined the biological importance of JNK-mediated PIN1 Ser115 phosphorylation in the response of ICC cells to ATRA. Compared with PIN1-depleted ICC cells reconstituted with rPIN1 WT, PIN1-depleted ICC cells reconstituted with rPIN1 S115A mutant were much less sensitive to ATRA-induced growth inhibition (Fig. 7G), implying that PIN1 Ser115 phosphorylation is crucial for the susceptibility of ICC cells toward ATRA.

Discussion

Activation of the JNK signaling pathway in cholangiocytes is a key event in cholangiocarcinogenesis and a promising target in ICC therapy.[8] However, due to its multifunctional role in liver homeostasis,[12-15] the development of selective therapies that target JNK directly are unlikely to result in clinically translatable options.[9,40,46] Therefore, understanding the mechanism through which JNK activation promotes ICC growth and the identification of downstream effectors as druggable targets are critical steps for expanding the therapeutic management of ICC. Here we uncover a mechanistic link between JNK activity and ICC cell proliferation through PIN1 protein stabilization and demonstrate the potential application of the PIN1 inhibitor ATRA for ICC therapy.

Elevated levels of PIN1 were found in ICC cell lines as well as ICC tissues, and positively correlated with the phosphorylation/activity levels of JNK proteins. Intriguingly, the positive association between JNK activity and PIN1 levels appears to be specific to ICC cells, as it was not observed in nontumoral human biliary epithelial cells, in which JNK kinase activities are not constitutively up-regulated. While blocking JNK activity led to a significant decrease in PIN1 protein levels, ectopic expression of a constitutively active form of JNK1 ($JNK1^{CA}$) led to an increase in endogenous PIN1 protein levels. Thus, PIN1 functions downstream of the JNK pathway, consistent with the established role of PIN1 in RAS signaling.[16,17,20]

PIN1 was first identified as a key regulator of cell division and later shown to promote tumorigenesis and tumor progression by inactivating proliferation-restraining factors or activating proliferation-promoting factors.[20-24] Consistent with the latter, we found that PIN1 is essential for proliferation of both cultured and xenografted ICC cells and functionally mimics JNK activation, thus reflecting the regulatory role of JNK activation on PIN1.

What then is the mechanism by which JNK activity regulates PIN1 expression? Activated JNK proteins regulate a variety of cellular processes, including proliferation, by acting on a number of nuclear and nonnuclear proteins at either transcriptional or post-translational levels.[9,40] We found that JNK activity regulates the intracellular PIN1 levels by stabilizing PIN1 through its phosphorylation, thus preventing PIN1 mono-ubiquitination and proteasomal

degradation. This is demonstrated by showing that the newly synthesized endogenous PIN1 displayed a shortened half-life in JNK-depleted or SP600125-treated ICC cells, and the decreased intracellular protein levels of PIN1 were reversed by the addition of the proteasome inhibitor MG132. In JNK-depleted ICC cells, the decrease in PIN1 levels was associated with the appearance of a mono-ubiquitinated form of PIN1, implying that JNK proteins inhibit the mono-ubiquitination of endogenous PIN1. Furthermore, JNK kinase activity is strictly required for such inhibition as overexpression of the constitutively active form of JNK1, but not its nonactive form, inhibited PIN1 mono-ubiquitination. Thus, in accordance with previous works showing that protein stability of PIN1 is regulated through the ubiquitin-proteasome system[34-36] and that small proteins are more likely to be mono-ubiquitinated rather than polyubiquitinated for degradation,[37,47] constitutive JNK activation prevents PIN1 mono-ubiquitination-induced proteasomal degradation, resulting in the stabilization and elevated levels of PIN1. In line with our finding that JNK activity is required for preventing PIN1 mono-ubiquitination, we show that JNK proteins directly interact with and phosphorylate PIN1 at Ser115, thus pinpointing PIN1 as a direct downstream target of JNK signaling. Moreover, we show that the reconstituted expression of non-phosphorylatable PIN1 S115A mutant, which was resistant to JNK-mediated suppression of PIN1 mono-ubiquitination, failed to revert impaired ICC cell growth. Therefore, the stabilization of PIN1 upon phosphorylation at Ser115 by active JNK represents a causal link between JNK activation and high PIN1 levels, and defines the JNK-PIN1 axis as essential for cholangiocarcinoma proliferation.

Given that PIN1 is aberrantly expressed at high levels in various types of tumor, including HCC, B-cell lymphoma, brain and lung cancer, in which constitutive JNK activation is commonly observed,[9,20,36] we speculate that the JNK-mediated stabilization of PIN1 may similarly contribute to the high expression of PIN1 in tumors of diverse tissue origin. Notably, many downstream effectors of the JNK pathway, such as c-Jun and cyclin D1, which promote cancer cell proliferation, are reported to be also regulated by PIN1.[9,17,20] Interestingly, we found that the reconstituted expression of PIN1(S115A) mutant but not that of rPIN1 WT failed to revert the levels/activities of key cell proliferation regulators in ICC cells. Thus, it is reasonable to hypothesize that JNK-mediated PIN1 Ser115 phosphorylation may significantly contribute to the pro-proliferative function of activated JNK in many human cancers.

Targeting downstream effectors in JNK signaling is a promising approach for inhibition of tumor proliferation in JNK-dependent tumors.[9,40,46] Our results point to PIN1 as a key downstream effector of the JNK pathway and show that the PIN1 inhibitor ATRA[36] effectively impaired ICC cell growth both in *in vitro* and xenograft experiments, with a corresponding decrease in PIN1 levels but not in JNK phosphorylation/activity. Although we cannot rule out that other mechanisms of action of ATRA[21,27] could also be responsible for its growth inhibitory effect in ICC cells, ATRA treatment in ICC cells phenocopies the effects of PIN1 knockdown. Thus, one would expect that ATRA may interfere with the JNK-PIN1 regulatory axis and block its oncogenic function in ICC, while leaving JNK activation unaffected.

The obvious question that remains to be addressed is how JNK-mediated Ser115 phosphorylation inhibits its PIN1mono-ubiquitination. In agreement with the notion that protein ubiquitination occurs primarily on highly solvent-exposed lysine residues,[42,43] we show that the Lys117 of PIN1 is the mono-ubiquitination site targeted for proteasomal degradation. Molecular dynamics simulations suggest that Lys117 displays a decreased solvent accessibility following phosphorylation at Ser115. Therefore, it is likely that JNK-mediated Ser115 phosphorylation may shield Lys117 from intermolecular interactions with components of the ubiquitination machinery by decreasing its surface exposure. Future investigations are warranted to address this question.

Our findings provide insights into the mechanisms by which constitutive JNK activation promotes cholangiocarcinoma growth and identify PIN1 as a direct downstream target of JNK, revealing an unexpected regulatory axis that sustains elevated PIN1 intracellular levels required for cell proliferation (Fig. 7H). We propose that targeting PIN1 using ATRA could be a potential therapeutic strategy for ICC. Rapid application of this strategy would be possible, as ATRA is a Food and Drug Administration–approved drug to treat APL[27] and is currently being clinically trialed for treatment of other solid cancers (ClinicalTrials.gov: NCT04113863).

Acknowledgment: The authors thank Ulf Klein (University of Leeds) for the insightful comments to the manuscript; Michael B. Yaffe (MIT Center for Precision Cancer Medicine) for the GST-PIN1 plasmid; J. Zhang (Duke University) for the $JNK1^{CA}$ and $JNK2^{CA}$; G. Franzoso (Imperial College London) for the c-Jun and shRNA lentiviral vectors; D. Trono (Ecole Polytechnique Federale de Lausanne, Switzerland) for the pWPI lentiviral vector; and D. Guardavaccaro (University of Verona) for the pWC7-His-Myc-Ubiquitin-WT, pCMV-His-HA-Ubiquitin-WT, and pWC7-His-Myc-Ubiquitin K0. They also thank L. Jary, D. Evans, and J. Bilton (University of Leeds) for the technical assistance.

Author Contributions: A.L., P.M.C., N.C.L., M.A.C., C.B., and S.P. performed most of the experiments. R.F., G.G., and M.L. helped with animal studies and data analyses. M.A.B-O. performed quantitative PCR. S.S.G. and G.A. provided essential reagents and helped with data analyses. C.D'S. performed mass spectrometry analyses. A.P. performed the computational modeling and interpretation. R.M.T. and W-K.S. helped with data analyses and interpretation. C.B. and S.P. are both senior and lead authors, conceived the idea, chiefly carried out data analysis and interpretation, coordinated and supervised the study, obtained research funding, and wrote the manuscript, which was commented by all the authors.

REFERENCES

1) Razumilava N, Gores GJ. Cholangiocarcinoma. Lancet 2014;383:2168-2179.
2) Khan SA, Thomas HC, Davidson BR, Taylor-Robinson SD. Cholangiocarcinoma. Lancet 2005;366:1303-1314.
3) Guest RV, Boulter L, Dwyer BJ, Forbes SJ. Understanding liver regeneration to bring new insights to the mechanisms driving cholangiocarcinoma. NPJ Regen Med 2017;2:13.
4) **Zou S**, **Li J**, **Zhou H**, **Frech C**, **Jiang X**, **Chu JS**, et al. Mutational landscape of intrahepatic cholangiocarcinoma. Nat Commun 2014;5:5696.
5) **Ikenoue T**, **Terakado Y**, Nakagawa H, Hikiba Y, Fujii T, Matsubara D, et al. A novel mouse model of intrahepatic cholangiocarcinoma induced by liver-specific Kras activation and Pten deletion. Sci Rep 2016;6:23899.
6) Robertson S, Hyder O, Dodson R, Nayar SK, Poling J, Beierl K, et al. The frequency of KRAS and BRAF mutations in intrahepatic cholangiocarcinomas and their correlation with clinical outcome. Hum Pathol 2013;44:2768-2773.
7) Tannapfel A, Benicke M, Katalinic A, Uhlmann D, Köckerling F, Hauss J, et al. Frequency of p16(INK4A) alterations and K-ras mutations in intrahepatic cholangiocarcinoma of the liver. Gut 2000;47:721-727.
8) Yuan D, Huang S, Berger E, Liu L, Gross N, Heinzmann F, et al. Kupffer cell-derived Tnf triggers cholangiocellular tumorigenesis through JNK due to chronic mitochondrial dysfunction and ROS. Cancer Cell 2017;31:771-789.
9) Bubici C, Papa S. JNK signalling in cancer: in need of new, smarter therapeutic targets. Br J Pharmacol 2014;171:24-37.
10) **Cellurale C**, **Sabio G**, Kennedy NJ, Das M, Barlow M, Sandy P, et al. Requirement of c-Jun NH(2)-terminal kinase for Ras-initiated tumor formation. Mol Cell Biol 2011;31:1565-1576.
11) Nielsen C, Thastrup J, Bøttzauw T, Jäättelä M, Kallunki T. c-Jun NH2-terminal kinase 2 is required for Ras transformation independently of activator protein 1. Cancer Res 2007;67:178-185.
12) Seki E, Brenner DA, Karin M. A liver full of JNK: signaling in regulation of cell function and disease pathogenesis, and clinical approaches. Gastroenterology 2012;143:307-320.
13) Solinas G, Becattini B. JNK at the crossroad of obesity, insulin resistance, and cell stress response. Mol Metab 2016;6:174-184.
14) **Cubero FJ**, **Mohamed MR**, Woitok MM, Zhao G, Hatting M, Nevzorova YA, et al. Loss of c-Jun N-terminal Kinase 1 and 2 function in liver epithelial cells triggers biliary hyperproliferation resembling cholangiocarcinoma. Hepatol Commun 2020;4:834-851.
15) Manieri E, Folgueira C, Rodríguez ME, Leiva-Vega L, Esteban-Lafuente L, Chen C, et al. JNK-mediated disruption of bile acid homeostasis promotes intrahepatic cholangiocarcinoma. Proc Natl Acad Sci U S A 2020;117:16492-16499.
16) Ryo A, Liou YC, Wulf G, Nakamura M, Lee SW, Lu KP. PIN1 is an E2F target gene essential for Neu/Ras-induced transformation of mammary epithelial cells. Mol Cell Biol 2002;22:5281-5295.
17) Wulf GM, Ryo A, Wulf GG, Lee SW, Niu T, Petkova V, et al. Pin1 is overexpressed in breast cancer and cooperates with Ras signaling in increasing the transcriptional activity of c-Jun towards cyclin D1. EMBO J 2001;20:3459-3472.
18) Wulf G, Garg P, Liou YC, Iglehart D, Lu KP. Modeling breast cancer in vivo and ex vivo reveals an essential role of Pin1 in tumorigenesis. EMBO J 2004;23:3397-3407.
19) Lu KP, Hanes SD, Hunter T. A human peptidyl-prolyl isomerase essential for regulation of mitosis. Nature 1996;380:544-547.
20) Zhou XZ, Lu KP. The isomerase PIN1 controls numerous cancer-driving pathways and is a unique drug target. Nat Rev Cancer 2016;16:463-478.
21) Pinch BJ, **Doctor ZM**, **Nabet B**, Browne CM, Seo HS, Mohardt ML, et al. Identification of a potent and selective covalent Pin1 inhibitor. Nat Chem Biol 2020;16:979-987.
22) Chen Y, Wu YR, Yang HY, Li XZ, Jie MM, Hu CJ, et al. Prolyl isomerase Pin1: a promoter of cancer and a target for therapy. Cell Death Dis 2018;9:883.
23) Pu W, Zheng Y, Peng Y. Prolyl isomerase Pin1 in human cancer: function, mechanism, and significance. Front Cell Dev Biol 2020;8:168.
24) Rustighi A, Zannini A, Campaner E, Ciani Y, Piazza S, Del Sal G. PIN1 in breast development and cancer: a clinical perspective. Cell Death Differ 2017;24:200-211.
25) **Jhaveri K**, **Teplinsky E**, Silvera D, Valeta-Magara A, Arju R, Giashuddin S, et al. Hyperactivated mTOR and JAK2/STAT3 pathways: molecular drivers and potential therapeutic targets of inflammatory and invasive ductal breast cancers after neoadjuvant chemotherapy. Clin Breast Cancer 2016;6:113-122.e1.
26) Gomez-Chou SB, Swidnicka-Siergiejko AK, Badi N, Chavez-Tomar M, Lesinski GB, Bekaii-Saab T, et al. Lipocalin-2 promotes pancreatic ductal adenocarcinoma by regulating inflammation in the tumor microenvironment. Cancer Res 2017;77:2647-2660.
27) Masetti R, Vendemini F, Zama D, Biagi C, Gasperini P, Pession A. All-trans retinoic acid in the treatment of pediatric acute promyelocytic leukemia. Expert Rev Anticancer Ther 2012;12:1191-1204.
28) **Tong Y**, **Ying H**, Liu R, Li L, Bergholz J, Xiao ZX. Pin1 inhibits PP2A-mediated Rb dephosphorylation in regulation of cell cycle and S-phase DNA damage. Cell Death Dis 2015;6:e1640.

29) Barbarulo A, Iansante V, Chaidos A, Naresh K, Rahemtulla A, Franzoso G, et al. Poly(ADP-ribose) polymerase family member 14 (PARP14) is a novel effector of the JNK2-dependent pro-survival signal in multiple myeloma. Oncogene 2013;32:4231-4242.
30) Iansante V, Choy PM, Fung SW, Liu Y, Chai JG, Dyson J, et al. PARP14 promotes the Warburg effect in hepatocellular carcinoma by inhibiting JNK1-dependent PKM2 phosphorylation and activation. Nat Commun 2015;6:7882.
31) Stebbing J, Shah K, Lit LC, Gagliano T, Ditsiou A, Wang T, et al. LMTK3 confers chemo-resistance in breast cancer. Oncogene 2018;37:3113-3130.
32) Alpini G, Invernizzi P, Gaudio E, Venter J, Kopriva S, Bernuzzi F, et al. Serotonin metabolism is dysregulated in cholangiocarcinoma, which has implications for tumor growth. Cancer Res 2008;68:9184-9193.
33) Bennett BL, Sasaki DT, Murray BW, O'Leary EC, Sakata ST, Xu W, et al. SP600125, an anthrapyrazolone inhibitor of Jun N-terminal kinase. Proc Natl Acad Sci U S A 2001;98:13681-13686.
34) Eckerdt F, Yuan J, Saxena K, Martin B, Kappel S, Lindenau C, et al. Polo-like kinase 1-mediated phosphorylation stabilizes Pin1 by inhibiting its ubiquitination in human cells. J Biol Chem 2005;280:36575-36583.
35) Basu A, Das M, Qanungo S, Fan XJ, DuBois G, Haldar S. Proteasomal degradation of human peptidyl prolyl isomerase pin1-pointing phospho Bcl2 toward dephosphorylation. Neoplasia 2002;4:218-227.
36) Wei S, Kozono S, Kats L, Nechama M, Li W, Guarnerio J, et al. Active Pin1 is a key target of all-trans retinoic acid in acute promyelocytic leukemia and breast cancer. Nat Med 2015;21:457-466.
37) Swatek KN, Komander D. Ubiquitin modifications. Cell Res 2016;26:399-422.
38) **Yuniati L**, **Lauriola A**, Gerritsen M, Abreu S, Ni E, Tesoriero C, et al. Ubiquitylation of the ER-shaping protein Lunapark via the CRL3KLHL12 ubiquitin ligase complex. Cell Rep 2020;31:107664.
39) Kinoshita E, Kinoshita-Kikuta E, Koike T. Separation and detection of large phosphoproteins using Phos-tag SDS-PAGE. Nat Protoc 2009;4:1513-1521.
40) Zeke A, Misheva M, Reményi A, Bogoyevitch MA. JNK signaling: regulation and functions based on complex protein-protein partnerships. Microbiol Mol Biol Rev 2016;80:793-835.
41) **Rangasamy V**, **Mishra R**, Sondarva G, Das S, Lee TH, Bakowska JC, et al. Mixed-lineage kinase 3 phosphorylates prolyl-isomerase Pin1 to regulate its nuclear translocation and cellular function. Proc Natl Acad Sci U S A 2012;109:8149-8154.
42) **Zhou Y**, **Liu S**, Song J, Zhang Z. Structural propensities of human ubiquitination sites: accessibility, centrality and local conformation. PLoS One 2013;8:e83167.
43) Catic A, Collins C, Church GM, Ploegh HL. Preferred in vivo ubiquitination sites. Bioinformatics 2004;20:3302-3307.
44) Ranganathan R, Lu KP, Hunter T, Noel JP. Structural and functional analysis of the mitotic rotamase Pin1 suggests substrate recognition is phosphorylation dependent. Cell 1997;89:875-886.
45) **Yin DL**, **Liang YJ**, **Zheng TS**, **Song RP**, Wang JB, Sun BS, et al. EF24 inhibits tumor growth and metastasis via suppressing NF-kappaB dependent pathways in human cholangiocarcinoma. Sci Rep 2016;6:32167.
46) Messoussi A, Feneyrolles C, Bros A, Deroide A, Daydé-Cazals B, Chevé G, et al. Recent progress in the design, study, and development of c-Jun N-terminal kinase inhibitors as anticancer agents. Chem Biol 2014;21:1433-1443.
47) **Shabek N**, **Herman-Bachinsky Y**, Buchsbaum S, Lewinson O, Haj-Yahya M, Hejjaoui M, et al. The size of the proteasomal substrate determines whether its degradation will be mediated by mono- or polyubiquitylation. Mol Cell 2012;48:87-97.

Author names in bold designate shared co-first authorship.

Supporting Information

Additional Supporting Information may be found at onlinelibrary.wiley.com/doi/10.1002/hep.31983/suppinfo.